

UCLA

UCLA Previously Published Works

Title

Influence of urbanization on winter surface temperatures in a topographically asymmetric Tropical City, Bhubaneswar, India

Permalink

<https://escholarship.org/uc/item/0xq3c7g9>

Journal

Computational Urban Science, 3(1)

ISSN

2730-6852

Authors

Nayak, Hara Prasad

Nandini, Gopinath

Vinoj, V

et al.

Publication Date

2023

DOI

10.1007/s43762-023-00112-y

Peer reviewed




ORIGINAL PAPER

Open Access



Influence of urbanization on winter surface temperatures in a topographically asymmetric Tropical City, Bhubaneswar, India

Hara Prasad Nayak^{1,2*} , Gopinath Nandini¹, V. Vinoj¹, Kiranmayi Landu¹, Debadatta Swain¹, Uma Charan Mohanty³ and Dev Niyogi⁴

Abstract

Urban areas experience significant alterations in their local surface energy balance due to changes in the thermal properties of impervious surfaces, albedo, land use, and land cover. In addition, the embedded influence of urbanization and heat-trapping in the urban canopy cause city temperature warmer compared to its surroundings peri-urban regions. However, the influence of urbanization on winter surface temperatures remains unclear. In this study, the urbanization influence on winter surface temperature in Bhubaneswar, a tropical two-tier city in India, is assessed using a high-resolution (4 km × 4 km) urban canopy model coupled with the Weather Research and Forecasting model. Numerical experiments are conducted with no urban coupling (CTL) and with coupling of a single-layer urban canopy model (UCM) for the winters of 2004 and 2015. The study suggests that both model simulations exhibit a similar warm bias in mean surface temperature (~2.2°C), but UCM's surface temperature better agrees with the observations compared to CTL. The warm bias in both experiments is primarily contributed by a higher nighttime warm bias (~3.2°C). The study reveals that urbanization contributes to ~0.4°C increase in surface temperature in 2015, especially in the eastern lowland regions of the city, while the impact is minimal in 2004. In the western region, the influence is nullified, possibly due to lower surface specific humidity affecting longwave radiation in a higher terrain setting. This study underscores the significance of terrain and local microclimate conditions in shaping winter urban surface temperatures, shedding light on the complex interplay between urbanization and climate.

Keywords Winter surface temperature, Urbanization, Urban canopy model, Topography

1 Introduction

The urban weather and climate are of growing concern in recent years due to the environmental issues affecting cities, such as floods, droughts, heat stress, and air pollution etc. Recent studies have highlighted the role of urbanization and human activities in exacerbating these issues (Li et al., 2021; Niyogi et al., 2020; Swain et al., 2023). Moreover, the urban population has been rapidly increasing in recent years. According to the World Urbanization Prospects 2014, approximately 54% of the global population lives in cities, and this is projected to increase to about 66% by 2050 (United Nations, Department of Economic and Social Affairs, Population Division, 2015). As cities grow, natural

*Correspondence:

Hara Prasad Nayak
hpnayak@ucla.edu

¹ School of Earth Ocean and Climate Sciences, Indian Institute of Technology Bhubaneswar, Bhubaneswar, India

² Department of Geography, University of California Los Angeles, Los Angeles, USA

³ Centre for Climate Smart Agriculture, Siksha 'O' Anusandhan Deemed to be University, Bhubaneswar, India

⁴ Jackson School of Geosciences, and Cockrell School of Engineering, University of Texas, Austin, USA



land is replaced by impervious urban surfaces, leading to changes in surface thermal properties and moisture feedback. These changes modify the surface energy and water budget over the urban region, altering the urban boundary layer processes, temperature (Li et al., 2018; Morris et al., 2016; Zhong et al., 2017), cloud (Zhong & Yang, 2015), rainfall (Kishtawal et al., 2010; Niyogi et al., 2020; Pielke Sr. et al., 2011), and affecting the regional climate (Arnfield, 2003; Jin et al., 2005; Kalnay & Cai, 2003; Kaufmann et al., 2007; Li et al., 2016; Zhou et al., 2004). Under future climate projections, weather and climate extremes, such as heat waves, droughts, floods, thunderstorms, and heavy rainfall events, are likely to become more frequent (Intergovernmental Panel for Climate Change (IPCC) 5th assessment report, 2014). These effects of global climate change, when combined with various urban boundary layer processes, make city populations more vulnerable to weather and climate extremes. Therefore, understanding the urban surface layer processes is imperative for predicting urban weather and mitigating the associated hazards.

The global temperature has risen by $\sim 1^\circ\text{C}$ compared to the pre-industrial era (IPCC fifth assessment report, 2014), with human activities being the primary contributor to this temperature rise due to the increasing anthropogenic emissions in the atmosphere (IPCC Fourth Assessment Report, 2007). The impact of anthropogenic activities is more pronounced in cities, which have higher population density and greater urbanization and industrialization. In addition, land use and land cover (LULC) changes also significantly affect regional and local surface temperatures (Grover & Singh, 2015; Mahmood et al., 2010; Niyogi et al., 2018). Previous studies have shown that LULC change has a clear influence on surface temperatures at both regional and local scales (Mohan et al., 2012; Mohan & Kandya, 2015; Nayak & Mandal, 2012; Swain et al., 2017). The impact of LULC change on surface temperatures is more evident in urban areas (Nandini et al., 2022). It has been widely documented that cities are generally warmer than the surrounding rural areas, which is referred to as the Urban Heat Island (UHI) effect (Arnfield, 2003; Grimmond, 2007; Oke, 1973; Zhao et al., 2014). This phenomenon is primarily caused by the impervious urban surface, building geometry, and street canyons, which trap outgoing longwave radiation and create a warmer microclimate. The Urban Heat Island (UHI) effect and its impacts have been studied extensively in many cities worldwide (Clinton & Gong, 2013; Estoque et al., 2017; Hunt et al., 2018; Imhof et al., 2010; Peng et al., 2012; Zhou et al., 2013). These studies have looked at various factors that contribute to the UHI effect, such as land use, surface materials, and anthropogenic activities, as well

as its effects on the urban environment, such as air quality, energy consumption, and human health.

The smart city of Bhubaneswar, the capital of the eastern state of Odisha in India, is also affected by urban heat stress. A recent observational study by Anasuya et al. (2019) found that the city's built-up area increased by 77% between 2003 and 2017, which resulted in an 8% increase in summer land surface temperatures. They also demonstrated that the city's temperature increased by 9.84% during the recent five-year period (2013–2017). Gogoi et al. (2019) used the observation minus reanalysis method to show that the Eastern state of Odisha experienced accelerated warming ($\sim 0.9^\circ\text{C}$) during recent decade (2001–2010), with 25–50% of the warming attributed to LULC change. Another modeling effort over Bhubaneswar revealed that urbanization is responsible for 60–70% of the overall increase in nighttime air temperature between 2004 and 2015 (Nandini et al., 2022). Swain et al. (2023) found that the timing of rainfall in the city is highly correlated with urban sprawl. However, modeling of urban surface processes is still in the incipient stage and require efforts to understand the urbanization influence on surface temperature, especially in winter (Ma et al., 2017; Sharma et al., 2021; Wang et al., 2021; Wang et al., 2023; Wu et al., 2021). Studies have demonstrated that winter surface temperatures exhibit a higher sensitivity ($2\text{--}3^\circ\text{C}$) to anthropogenic heat flux compared to summer surface temperatures ($1\text{--}2^\circ\text{C}$) (Fan & Sailor, 2005; Feng et al., 2012; Ichinose et al., 1999). Furthermore, the change in surface temperature due to the effect of anthropogenic heat flux depends on atmospheric stratification and orographic factors (Block et al., 2004; Narumi et al., 2009; Zhang et al., 2016). The thermal stratification during winter nights prevents the dissipation of anthropogenic heating into the atmosphere, thereby contributing to about 90% of the Urban Heat Island (UHI) effect (Ma et al., 2017). Moreover, the study region experiences a dry winter climate with the lowest rainfall occurrence, and thereby the associated cooling or warming effect on surface temperature is assumed to be minimal during the season. Furthermore, there have been limited studies conducted to understand the interplay between urbanization and climate that influences winter surface temperatures (Wang et al., 2021; Wu et al., 2021). The present work focuses on studying the urbanization effect on the winter surface temperatures of Bhubaneswar city.

Most numerical weather prediction (NWP) models do not explicitly account for urban canopy layer exchange processes. The current state-of-the-art land surface models (LSMs) are not adequately representing the thermal exchange processes that occur within the impervious

city surface, building structures, street canyons, and heat transfer in walls, roofs, and streets. To incorporate urban surface feedback in NWP models, one of the common efforts is to incorporate the thermal properties of the impervious surface in the slab model. The slab model considers urban geometry as flat surfaces with modified thermal properties. However, the effect of building geometry, such as building coverage ratio, and physical constant of urban structures such as buildings, roads, street canyons, etc., have considerable influence on surface energy balance and therefore needs to be suitably parameterized in the NWP models. To this end, considerable efforts have been made to parameterize the urban canopy layer over the city (Arnfield et al., 1998; Johnson et al., 1991; Masson, 2000; Mills, 1993). Subsequently, a single-layer urban canopy model (SUCM; Kusaka et al., 2001; Kusaka & Kimura, 2004) is developed and has been successfully coupled with mesoscale atmospheric models (ARW/UCM) (Chen et al., 2004; Miao et al., 2009). The ARW/UCM has been applied to various cities around the world (Chen et al., 2011; Patel et al., 2022), including Indian cities, to study rainfall characteristics (Niyogi et al., 2020; Swain et al., 2023) and surface temperature (Mohan et al., 2020). However, urban feedback to the atmosphere is influenced by various factors such as the

city’s thermal properties, climate, and urban morphology. Therefore, it is necessary to conduct a city-specific assessment of the ARW/UCM system to accurately simulate surface temperature. This is because each city has unique characteristics that can affect the way urban areas interact with the atmosphere, and these characteristics need to be considered.

In this study, we utilized a high-resolution single-layer urban canopy model coupled with the Weather Research and Forecasting model (ARW/UCM) to understand the urbanization response to city winter surface temperature. To study the urbanization effect, two winter seasons are considered: 2004 and 2015. The model simulated temperature is verified with observation and further analysis carried out to understand urbanization influence on city surface temperature. The study has implications for city planners and mitigation efforts, as well as future modeling efforts that seek to address urban-induced heat stress.

2 Bhubaneswar geography and climate

Bhubaneswar is the capital city of the state of Odisha, located in the coastal region approximately 40 km west of the north Bay of Bengal (Fig. 1). The city is surrounded by the Chandaka Forest in the west, the

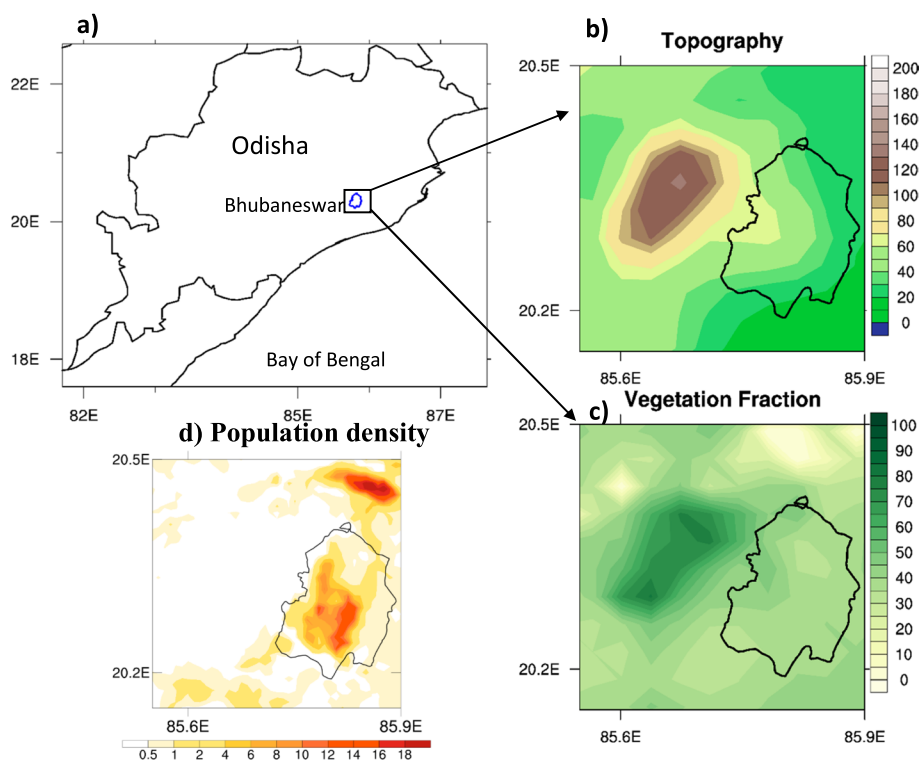


Fig. 1 a Geographical location of Bhubaneswar city, the capital of the eastern state Odisha, India. b, c & d) represents the topography (m), vegetation fraction (%) and population density (number of persons per square kilometer) $\times 10^3$ around the city, respectively

Kuakhai River (a tributary of the Mahanadi River) in the east, the Mahanadi River to the north, and agricultural land to the south. It has a unique topographical west-east asymmetric feature, with upland areas (~180 m above sea level) in the west and lowland areas in the east (~20 m in the east-southeast), and benefits from a natural drainage with the ground sloping from west to east (Fig. 1b). The city has an average elevation of 45 m above sea level. The city's population is approximately 8.43 lakhs, according to the 2011 census report from the Government of India, and it covers an area of around 233 sq. km.

The population density mostly confined over the center of the city with maximum density $\sim 16 \times 10^3$ (Fig. 1d). The vegetation fraction over the city is around 30–40% (Fig. 1c). The city belongs to the moderately humid tropical climate zone, with a maximum temperature of around 44°C, a minimum temperature of around 12°C, and an annual rainfall of 1498 mm.

3 Data and methodology

In the present study, a regional climate modeling system, the Weather Research and Forecasting model (ARW v4.0) (Skamarock et al., 2008), is used for the simulation of winter temperature over Bhubaneswar city in India. In order to accommodate the urban surface exchange processes, a single-layer urban canopy model (SUCM; Kusaka & Kimura, 2004) coupled with ARW is used (hereafter referred to as UCM). The SUCM is designed to incorporate the surface energy balance modification due to city surface properties such as thermal conductivity, heat capacity, and surface albedo, along with roughness length, soil moisture availability, and city geometry, including street canyons. However, the present study is limited by the lack of detailed information about local thermal properties and urban morphology. The SUCM represents urban geometry as two-dimensional street canyons with infinite length, but considers the three-dimensional nature of urban morphologies, including the shadowing from buildings and the reflection of radiation in the canopy layer. The SUCM calculates the prognostic variables such as surface skin temperature and heat fluxes produced from urban facets (building roofs, walls, and roads). The fraction of impervious surface in a grid cell is represented by the urban fraction parameter through which the SUCM coupling is carried out. The surface fluxes over the impervious surface are calculated by the SUCM, whereas the LSM calculates fluxes over the vegetated fraction of the grid cell. The total grid cell surface flux is calculated as the weighted average of their respective fractional coverage.

The ARW/UCM model is configured with three nested domains: outer, middle, and inner domains at 36 km,

12 km, and 4 km grid spacing, respectively, surrounding Bhubaneswar city. The x-y dimensions of the outer, middle, and inner domains are (80×80), (100×100), and (61×61), respectively. The model uses 61 log-linear vertical pressure (sigma) coordinates with the Arakawa C-grid structure. The parameterization schemes used in the model include: the Boulac (Bougeault & Lacarrere, 1989) scheme for the planetary boundary layer, the community Noah-MP (Niu et al., 2011) scheme for the land surface, the Dudhia scheme for shortwave radiation (Dudhia, 1989), the Rapid Radiative transfer model scheme for longwave radiation (Mlawer et al., 1997), the WSM-6 scheme for microphysics (Hong & Lim, 2006), and the Kain-Fritsch scheme (Kain, 2004) for convection.

Numerical experiments are conducted for winter (DJF) seasons in 2004 and 2015 using the ARW model. These two winter seasons are selected depending on the availability of local land use data. Moreover, preliminary studies suggest that Bhubaneswar city has undergone urbanization after 2000, and the city has undergone considerable urbanization in recent years (Nandini et al., 2022). Therefore, consideration of 2004 and 2015 are reasonable for studying the urbanization influence on surface temperature. For each year season, two land surface sensitive experiments are carried out using: 1) no urban coupling (hereafter referred to as CTL) and 2) a single-layer urban canopy model coupled with the ARW model (hereafter referred to as UCM). Besides these changes, the rest of the model configurations remained the same in both experiments. The initial and the boundary conditions at 6-hourly temporal frequency are provided from NCEP final analysis ($1^\circ \times 1^\circ$). The local 19-category land use classification data is provided from National Remote Sensing Centre, India (National Remote Sensing Centre, India, 2008). This land use data is estimated at 56 m horizontal resolution, which is further rescaled to 30 arc sec (~ 0.925 km) and provided to the model. The soil and vegetation at the 30 arc sec are provided by the United States Geographical Survey (USGS) (Reynolds et al., 2000). The model simulated air Temperature at 2 m (T2) is validated with the hourly in-situ measurements at Bhubaneswar airport (20.25°N, 85.80°E). Besides, the study uses the city population data from Worldpop (<https://www.worldpop.org/>).

Figure 2 depicts the land use classification for the years 2004 and 2015 over Bhubaneswar city. The figure shows that Bhubaneswar has undergone substantial LULC change during the period 2004–2015. The LULC changes are observed mainly in two dominant land use classifications, such as (1) built-up/ urban land and (2) dryland cropland pasture. The built-up/urban area increased by $\sim 166\%$ during the period 2004–2015, followed by dryland cropland and pasture ($\sim 39\%$) (Table 1). The increase in the built-up area is primarily due to dryland

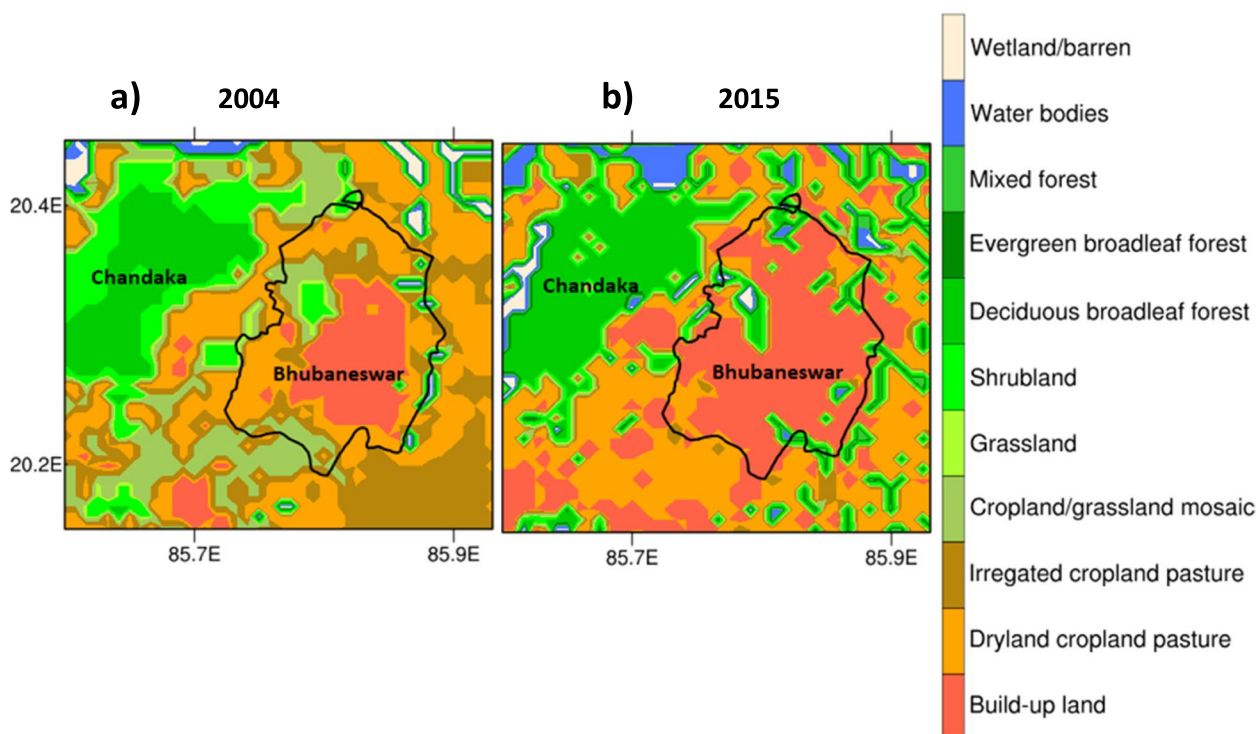


Fig. 2 Land use classifications over the Bhubaneswar city for the year **a)** 2004 and **b)** 2015

Table 1 The number of grid boxes for each land use classification is presented for the year 2004 and 2015. The percentage of change during the period 2004–2015 for each classification type is presented. There is total 3600 (60×60) grid points in domain 3, out of which the number of grids under each classification is tabulated

| Land use classification | Number of grid boxes (in 2004) | Number of grid boxes (in 2015) | % Change |
|------------------------------|--------------------------------|--------------------------------|----------|
| Urban and built-up land | 21 | 56 | 166.7 |
| Dryland cropland and pasture | 1134 | 1577 | 39.1 |
| Irrigated cropland pasture | 304 | 206 | −32.2 |
| Cropland grassland mosaic | 386 | 31 | −92 |
| Shrubland | 155 | 1 | −99.3 |
| Deciduous broadleaf forest | 615 | 697 | 13.3 |
| Evergreen broadleaf | 6 | 4 | −33.3 |
| Mixed forest | 5 | 25 | 400 |
| Water bodies | 933 | 933 | 0 |
| Wooden wetland | 3 | 1 | −66.6 |
| Barren or sparsely vegetated | 38 | 69 | 81.6 |

transformations into build-up land. A similar transformation from irrigated cropland/grassland to dryland is also seen. Overall, the analysis indicates that the built-up and dryland area increased in 2015 at the expense of vegetated grassland /dryland compared to 2004. Such change in LULC could influence the city surface temperature, and the same is investigated through the city scale numerical modeling framework presented in the subsequent section.

4 Results and discussions

The model simulated near-surface temperature and 10m wind are analysed for Jan-Feb (JF) considering the first month (Dec) of simulation as model spin-up. The T2 simulation is verified against the AWS observation at Bhubaneswar. Note that the T2 verification is limited to only one station due to a lack of station observation over the city. Further analysis pertaining to

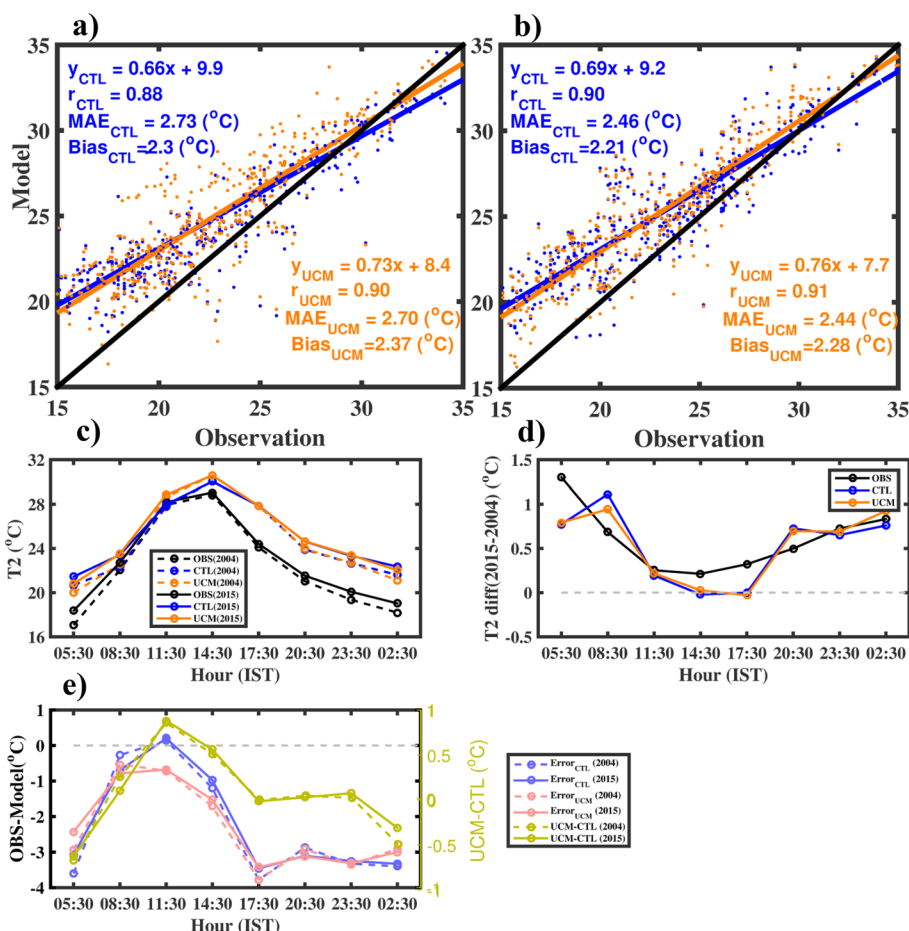


Fig. 3 Validation of model simulated 2 m Temperature (T2) at Bhubaneswar airport AWS station. **a** Represents the scatter diagram of the model simulated 3-hourly T2 from CTL (blue dots) and UCM (orange dots) against observation during Jan-Feb, 2004. The black line represents the $y=x$ line. The blue line (CTL) and orange line (UCM) represent the linear regression fit of the model simulated T2 against observation. The error statistics for the CTL experiment are provided at the top left corner of the figure, while for the UCM experiment, the error statistics are presented at the bottom right corner. **b** Represents the same as a) but for the year 2015. **c** Represents the diurnal variation of model simulated T2 from CTL, UCM and observation for Jan-Feb 2004 and 2015. **d** Represents the T2 difference between 2015 and 2004 from observation, CTL and UCM. **e** Represents the error in CTL and UCM simulations for both 2004 and 2015 as well as the difference between UCM and CTL simulations

near-surface temperature characteristics and associated UHI effects is carried out.

4.1 Validation of T2

The model simulated 3-hourly T2 is validated against observations at Bhubaneswar airport (20.25 °N, 85.80 °E) station during JF 2004 and 2015 (Fig. 3). The least squares linear regression fit ($y=mx+c$) of the model simulated T2 against observations is better in the UCM experiment ($m=0.73$) than in the CTL experiment ($m=0.66$) during JF 2004 (Fig. 3a). The correlation coefficient (r) and Mean Absolute Error (MAE) in the UCM experiment ($r=0.90$, $MAE=2.7$ °C) also showed slightly better agreement with observations than the CTL experiment ($r=0.88$, $MAE=2.7$ °C). However, mean biases were

found to be similar in both CTL (bias= 2.3 °C) and UCM (bias= 2.3 °C) experiments. The simulation of T2 during JF 2015 is consistent with 2004 in both UCM and CTL experiments (Fig. 3b). But the simulation skill is marginally improved in both UCM ($m=0.76$; $c=7.2$) and CTL ($m=0.69$; $c=9.2$) experiments. The verification of model simulation with observation reveals that the T2m is better simulated in UCM experiment as compared to the CTL.

4.1.1 Diurnal variation of temperature

Figure 3c shows the diurnal variation of observed T2 (black lines) at Bhubaneswar compared with CTL (blue line) and UCM (orange line) experiments of 2004 (dotted lines) and 2015 (thick lines). From observations, it

is seen that the maximum temperature (T_{\max}) rises by 0.2°C in 2015 (mean $T_{\max}=29.0^{\circ}\text{C}$) as compared to 2004 (mean $T_{\max}=28.8^{\circ}\text{C}$). Whereas the minimum temperature (T_{\min}) rises by 1.37°C in 2015 (mean $T_{\min}=18.37^{\circ}\text{C}$) as compared to 2004 (mean $T_{\min}=17.0^{\circ}\text{C}$). Moreover, T2 during late afternoon to early morning is notably higher in 2015 as compared to 2004 whereas, the daytime T2 remains similar. The cause of such a rise in T2 is a matter of further investigation. One of the primary causes is likely due to the contribution from LULC change, as reported in many previous studies (Gogoi et al., 2019; Nandini et al., 2022). However, such a rise of T2 is not only attributable to the LULC change; rather, the contribution of the urban canopy cannot be ignored.

The simulated T2 performed better during the daytime (8:30–14:30 IST), while the bias increased in the late afternoon and night with a bias of $\sim 2\text{--}3^{\circ}\text{C}$ in both CTL and UCM. The T2 bias is higher at night ($\sim 3.2^{\circ}\text{C}$) than during the day ($\sim 1.3^{\circ}\text{C}$). This T2 bias is likely attributed to uncertainty in Noah-MP LSM, as reported in a recent study by Patel et al. (2022), which demonstrated that Noah LSM could better simulate T2 than Noah-MP. Their study also suggests that the utilization of more detailed urban classification, such as local climate zone data, could further enhance T2 simulation. When comparing both sensitive experiments, the UCM experiments showed a warmer Tmax (by $\sim 0.5^{\circ}\text{C}$) and cooler Tmin (by 0.6°C) than the CTL experiment. As a result, the mean T2 bias remained the same ($\sim 2.2^{\circ}\text{C}$) in both experiments. Both model simulations could replicate the observed diurnal variation. Furthermore, the simulated T2 standard deviation is lower ($\sim 1.6^{\circ}\text{C}$ to 2.8°C) compared to the observation (2.5°C to 3.5°C) during the day, indicating a deficiency in the model's ability to replicate the observed variability. The T2 simulation at 17:30 IST and 08:30 IST also has limitations in replicating the observed variability, highlighting the need for further analysis of surface energy partitioning.

Figure 3d shows the diurnal temperature difference between 2015 and 2004 for observation, CTL, and UCM experiments. The observation indicates warmer T2 in 2015 compared to 2004 during the entire day. The T2 warming is higher during the early morning (1.37°C) and nighttime (increase by $\sim 0.7^{\circ}\text{C}$), whereas daytime warming is modest. These inferences are clear indications of the rapid urbanization of Bhubaneswar city. Interestingly, the model simulation followed the observed T2 difference except at 08:30 and 20:30 IST. Nevertheless, UCM simulated T2 difference better followed the observation. Figure 3e depicts the error in the model simulations and the T2 differences due to the sensitive experiments (UCM-CTL). The T2 simulation has a maximum error ($\sim -3.5^{\circ}\text{C}$) at 17:30 and 05:30 IST, and the least error (\sim

-0.5 to 0.2°C) at 08:30 and 11:30 IST. In these instances, the observation shows higher variability, and model simulation has limitations in replicating such variability. In general, the errors are higher ($\sim -3^{\circ}\text{C}$) during night than in day time. Note that the T2 difference due to the UCM experiment is notable during the early morning ($\sim -0.6^{\circ}\text{C}$) and during mid-day ($\sim 0.5^{\circ}\text{C}$). But the T2 difference is the least from 17:30 to 23:30. The errors in both simulations are likely attributed to the uncertainty in the LSM. In general, UCM shows cooling during the early morning and warming during the mid-day. Besides, the effect of surface energy partitioning on the T2 simulation is investigated further.

The preliminary analysis suggests that the T2 difference due to sensitive experiments is attributed to the surface longwave downward radiation partitioning, particularly during the night time. Figure 4 demonstrates the relationship between T2 difference and surface downward solar and thermal radiation difference due to the UCM-CTL. It shows that the T2 difference is linearly related to surface longwave downward radiation difference, whereas shortwave downward radiation does not exhibit such a relationship. Previous studies (Sugawara & Takamura, 2006) have also highlighted the importance of longwave radiation flux from the urban canopy in determining T2. However, further analysis regarding the canopy layer radiation partitioning is limited by the lack of radiation observation.

4.2 Effects on surface temperature

The comparison of the model simulated T2, along with 10 m wind, between CTL and UCM experiments of 2004 and 2015 is depicted in Fig. 5. The figure shows that the urban region (especially the built-up areas) has higher T2 in both CTL and UCM experiments. The T2 is $\sim 2.0^{\circ}\text{C}$ higher in the city than in the surrounding peri-urban regions, and the higher T2 zone expanded in 2015 following the city's expansion. In 2004, the UCM simulation did not show any significant change in T2 compared to the CTL experiment (Fig. 5c). However, the UCM simulation for 2015 exhibited warmer T2, particularly in the eastern part of the city, which is $\sim 0.4^{\circ}\text{C}$ higher than the CTL simulation (Fig. 5f). The T2 warming followed the lowland regions of the city, as shown in Fig. 1. The cause of T2 warming in the UCM experiments is likely attributed to downwelling longwave radiation partitioning at the surface. Note that the region is complex with west-east inclined terrain and vegetation. The winter temperature varies following the topography and moisture distribution. In addition, downwelling longwave radiation is also influenced by the terrain. Study by Pluss and Ohmura (1997) provided

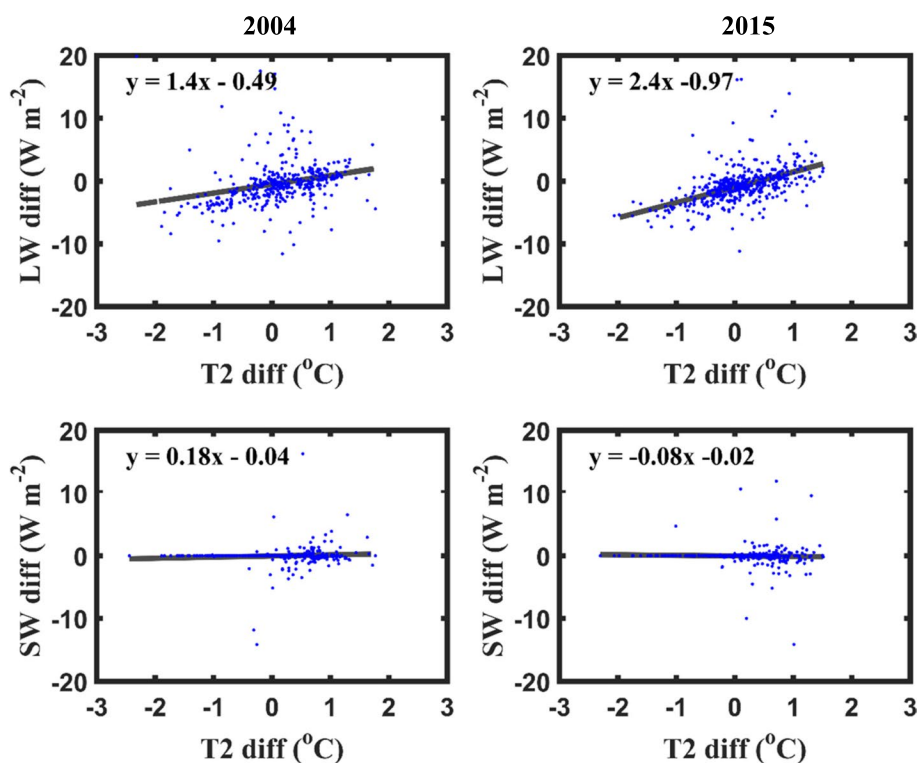


Fig. 4 Relation between surface temperature simulation and downward LW and SW radiation partitioning in both CTL and UCM simulations

expression for the downwelling LW radiation over the complex terrain as provided in eq. (1)

$$LW^\downarrow = La^\downarrow + Ls^\downarrow \tag{1}$$

Where L_a^\downarrow and L_s^\downarrow is the long wave radiation contributed by the atmosphere and terrain respectively. LW^\downarrow is the downwelling longwave radiation. Further, L_a^\downarrow is function of the near-surface humidity and near-surface air temperature (Brutsaert (1975). Recent studies have demonstrated that near-surface humidity and near-surface air temperature have a second-order effect on longwave radiation (Feldman et al., 2022). Specifically, the surface specific humidity and air temperature are higher in the east compared to the west of the city, and downward radiation is sensitive to these parameters, especially to specific humidity (Chen et al., 2014). Longwave radiation sensitivity is generally higher when specific humidity is lower (Chen et al., 2014). Moreover, this sensitivity is more pronounced in winter than in summer (Naud et al., 2013). In addition, downwelling longwave radiation sensitivity is smaller at lower altitudes and higher humidity due to the saturation of longwave absorption in the atmospheric window (Ruckstuhl et al., 2007). Figure 6 displays the difference in specific humidity (Q2) due to the UCM-CTL experiment. The drier specific humidity

in the UCM experiment likely influences the partitioning of downwelling longwave radiation, with greater sensitivity to the west due to lower specific humidity levels, thereby mitigating the urbanization influence in the west. The drier specific humidity over the urban region compared to rural region is called Urban Dry Island (UDI) effect and the phenomena is observed over various parts of the world (Meili et al., 2022). This UDI effect depends on various factor such as temperature, surface feedback due to the impervious urban surface and the moisture advection etc. However, understanding the UDI effect and its impact on urban energy and water balance is beyond the scope of this work. Additionally, Fig. 4 illustrates the difference in T2 due to the UCM experiment, which is linearly related to downwelling longwave radiation, supporting this relationship. Note that the moisture distribution over the region is very complex, influenced by various factors including urban-rural moisture differences, topography, vegetation, and sea-land breeze circulation. Our understanding of this phenomenon is still in its early stages and requires further investigation.

In addition, Fig. 5g and h also depict the T2 difference between 2015 and 2004 for the CTL and UCM experiments, respectively. The results show that the mean T2 is significantly warmer in 2015 than in 2004. The northern and southern parts of the city experienced the highest

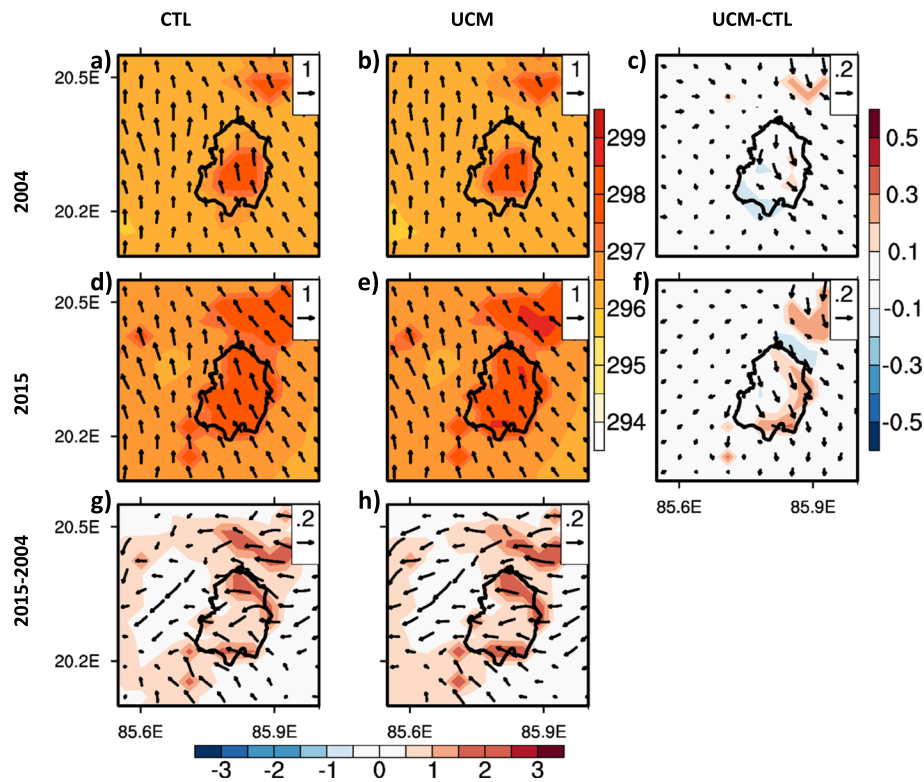


Fig. 5 Comparison of model simulated mean (JF) T2 between CTL and UCM simulations. The mean (JF) T2 from **a)** CTL, **b)** UCM experiments and **c)** their difference (UCM-CTL) for the year 2004 represented in first row. **d-f)** Represents same as (a-c) but for the year 2015. **g)** Represents mean T2 difference between 2015 and 2004 from the CTL simulation and **h)** represents same as g) but for UCM simulation

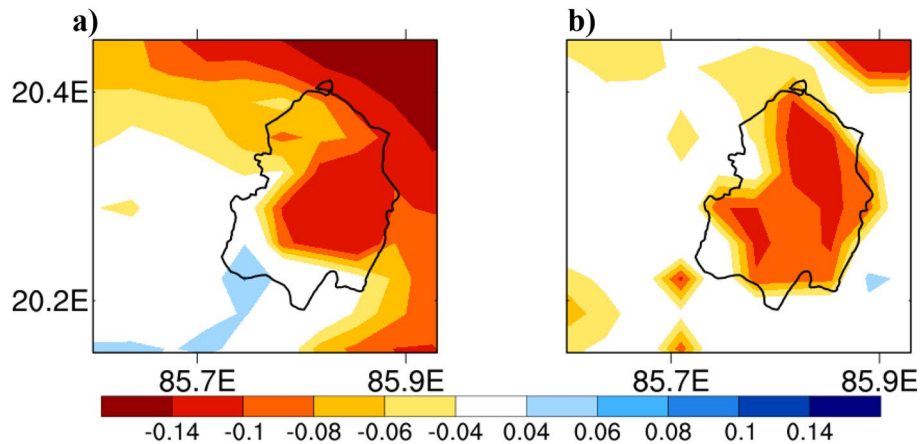


Fig. 6 The specific humidity difference (g/kg) due to UCM-CTL in **a)** 2004 and **b)** 2015

warming, with temperature increases of 2–3°C, while the central part of the city experienced a modest increase of approximately 0.5–1°C. This rise in T2 is likely contributed by the LULC change. Notably, the Chandaka Forest region has the smallest T2 increase (~0.3°C), indicating that vegetation cover can mitigate heat stress. The 10 m wind simulation showed that the prevailing surface wind

direction in both CTL and UCM experiments is southeasterly, with a speed of approximately 1 m/s. Interestingly, the UCM experiment exhibited a 0.2 m/s decrease in wind speed compared to the CTL experiment, likely due to higher surface roughness (Cao & Lin, 2014). This decrease in wind speed is particularly noticeable in the lowland eastern part of the city. When comparing

the wind simulations between 2015 and 2004, changes in wind direction and speed are evident. For instance, westward winds are observed in 2015 (Fig. 5g & h) compared to 2004, and the wind speed is also increased (by $\sim 0.3\text{ms}^{-1}$) in 2015. It is important to note that such changes in wind speed and direction in recent years may have consequences on city weather activities, particularly the pre-monsoon (March–May) thunderstorm activities over the city. The increase in wind speed, together with warmer temperatures over the city surface, could

influence convection and local land-sea breeze activities. A recent study by Swain et al. (2023) suggests increases in winter and pre-monsoon precipitation intensity over Bhubaneswar in recent years, with the precipitation time shift and spatial reorganization linked with urbanization. It is important to note that the present study only focuses on the winter (JF) season, and further studies are needed to investigate the potential impact of changes in wind speed and direction on convective activity over the region.

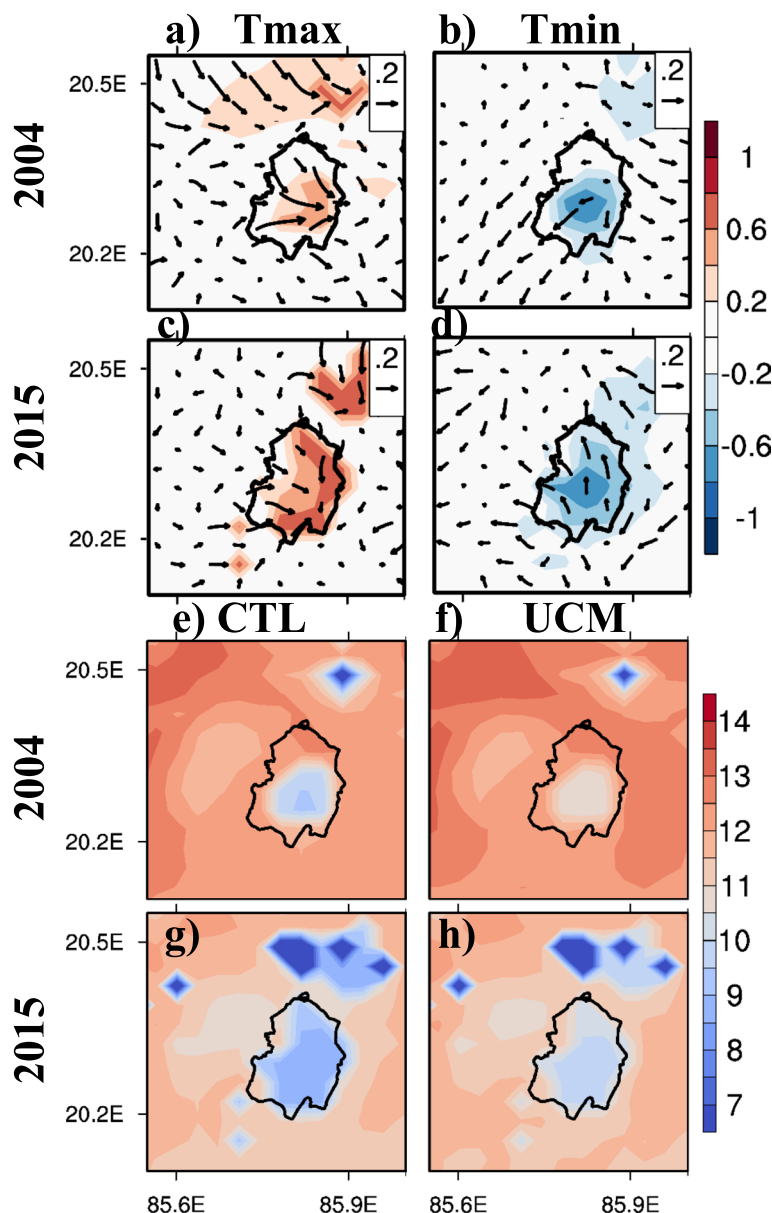


Fig. 7 The JF mean difference in Tmax between UCM and CTL experiments. **a** Represents the JF mean Tmax difference (UCM-CTL) with 10 m wind difference in the year 2004. **b** Depicts same as a) but for Tmin. **c, d** Represents same as a)-b) but for the year 2015. **e** and **f** represents diurnal temperature range for CTL and UCM experiment, respectively for the year 2004. **g, h** are same as **e-f**) but for the year 2015

Figure 7 displays the differences in Tmax, Tmin, 10 m wind, and diurnal temperature range (DTR) between the UCM and CTL experiments. The UCM experiment shows a warmer Tmax (by 0.5–1.0°C) than the CTL experiment, whereas Tmin is cooler by ~0.6°C. Additionally, the south-easterly wind over the city is weakened by 0.2 ms⁻¹ in the UCM simulation.

It is worth noting that the north-easterly wind at night may cause cold air advection from the Chandaka Forest regions, while the decrease in daytime wind speed could limit the warm air advection from the city. The DTR is increased by ~2°C in the UCM experiment compared to the CTL experiment. However, the DTR is found to be much higher (2°C - 4°C) in the peri-urban region than the urban region, as seen in both CTL and UCM experiments.

4.3 Urban Heat Island effect

The urban and peri-urban temperature difference (ΔT) surrounding the Bhubaneswar city is calculated, and the diurnal distribution of ΔT is presented in Fig. 8. The UHI differs due to the sensitive experiments during the day, whereas the nighttime UHI remains similar among sensitive experiments. However, the UHI magnitude is weaker during the day as compared to the night. This finding corroborates with prior studies (Eastin et al., 2018; Yang et al., 2013) conducted for other cities. The UHI

magnitude is higher in 2015 compared to 2004, especially at nighttime, with UHI values of approximately 2.6°C and 1.6°C in 2015 and 2004, respectively. Similar high nighttime UHI (2.7°C) is also found over South China (Li et al., 2021). However, the UHI difference due to the UCM - CTL is least at night. The daytime UHI is higher in the UCM simulation by 16% and 20% as compared to the CTL simulation in 2004 and 2015, respectively. Overall, the UHI effect comparatively lower in 2004 with UHI values 1.21°C and 1.25°C in the CTL and UCM simulations, respectively. Whereas, the UHI values are increased to 1.62°C and 1.77°C for CTL and UCM, respectively in 2015. The rise in UHI during 2015 as compared to 2004 suggest the rapid urbanization of the Bhubaneswar city.

5 Summary

In this study, we assess the influence of urbanization on winter surface temperature in the rapidly growing, topographically west-east asymmetric city of Bhubaneswar, India. We utilize a state-of-the-art regional climate modeling system coupled with the single-layer urban canopy model (ARW/UCM). Bhubaneswar has experienced significant population growth, economic development, and expansion of urban and built-up areas over the past two decades. Notably, there is a substantial increase in the built-up area from 2004 to 2015, at the expense of dryland and irrigated cropland/

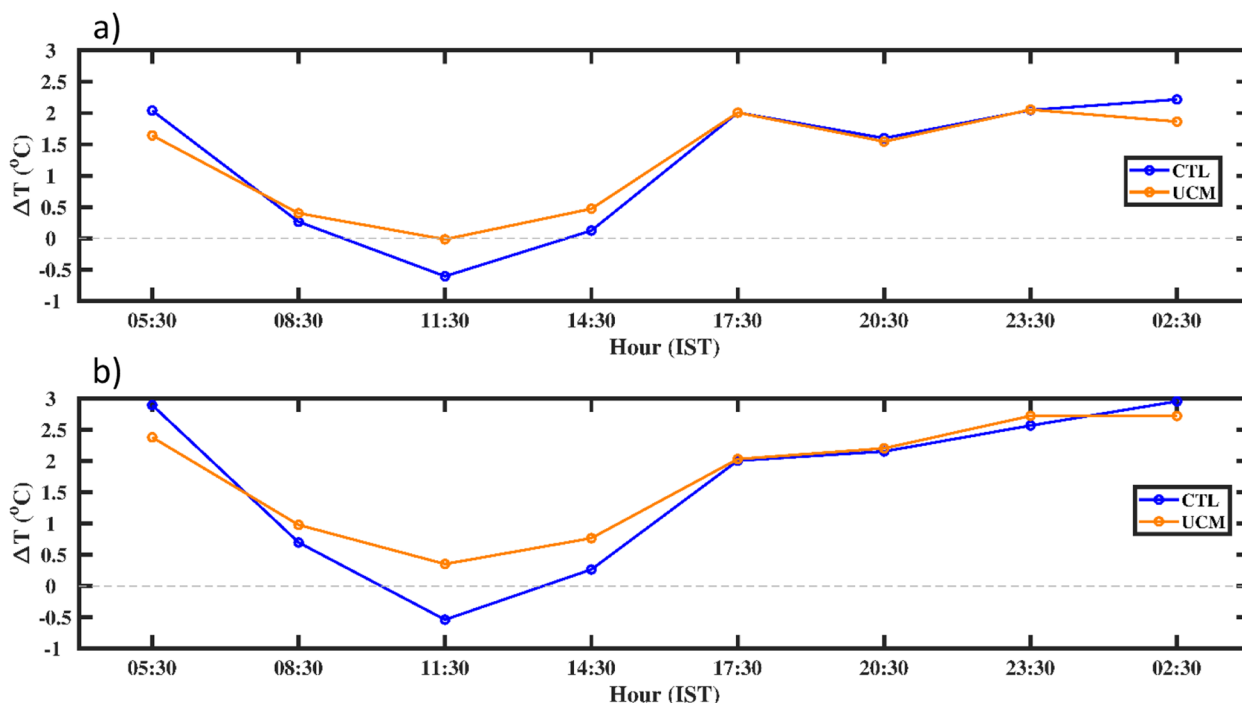


Fig. 8 Diurnal distribution of Urban Heat Island (UHI) effect of Bhubaneswar city obtained from CTL and UCM experiments of winter a) 2004 and b) 2015

grassland, which could affect the surface energy balance and, consequently, surface temperature. To study the impact of urbanization on winter temperature, we selected two winter seasons, 2004 and 2015, and conducted two numerical experiments for each season: 1) with no SUCM coupling (CTL) and 2) with SUCM coupling (UCM) using the atmospheric model (ARW). We employed local land use data from AWiFS for each seasonal simulation.

The model simulated T2 matches reasonably with observations in both CTL and UCM experiments, with a mean bias of approximately 2.2°C in both 2004 and 2015. However, the UCM simulated T2 shows better skill than CTL in both years. The T2 mean bias is primarily contributed by a high nighttime bias (~3.2°C). Both CTL and UCM experiments demonstrate warmer winter surface temperatures (1.5–2.0°C higher) over the city compared to the peri-urban region in both 2004 and 2015. The warmer temperature region expanded in 2015 following urban/build-up area expansion. In 2015, the UCM simulated T2 is ~0.4°C warmer than in the CTL experiment, particularly in the eastern lowland regions of the city. This warming is likely attributed to downward longwave radiation partitioning. However, this effect is negated in the west, likely due to lower surface-specific humidity at relatively higher terrain affecting downward longwave radiation. It's worth noting that the relationship between surface-specific humidity and downward longwave radiation is non-linear (Chen et al., 2014), especially over the higher terrain regions, and further investigation is necessary to confirm this relationship in tropical regions. Moreover, it is noteworthy to investigate the effect of urbanization on surface temperature in other regions with similar geographical settings.

Besides, both simulations show a notable rise in winter surface temperature during 2004–2015, especially in the city expansion regions, where T2 increased by 2–3°C. This temperature rise may be attributed to various factors, including climate change embedded with urbanization and LULC change etc.

This study underscores the significance of terrain and local climate in modulating the urbanization effect on winter surface temperatures in Bhubaneswar, India. It represents a preliminary effort in demonstrating the impact of urbanization on winter surface temperature. We acknowledge uncertainties in the land surface simulation, resulting in warm surface temperature bias, particularly at night. One caveat of the study is that it considers only two seasons for investigating the urbanization effect. Additionally, our study is limited by the use of non-local thermal properties for city surfaces. Future research that considers sub-urban classes

and use of sophisticated urban canopy parameterization may improve the city's surface energy balance and, consequently, enhance simulations of city surface temperatures.

Acknowledgements

VV and KL acknowledge support from the Department of Science and Technology climate change program (DST-SPLICE: DST/CCP/NUC/148/2018), Govt of India. Dr. Dev Niyogi is a Section Editor for the Computational Urban Science and was not involved in the editorial review, or the decision to publish, this article. All authors declare that there are no competing interests. The authors are thankful to the anonymous reviewer for their constructive suggestions and comments.

Code availability

The ARW model source code is freely available at https://www2.mmm.ucar.edu/wrf/users/download/get_source.html. The analysis is carried out using NCL (<https://www.ncl.ucar.edu/>) and matlab 2021a (<https://in.mathworks.com/>).

Authors' contributions

Conceptualization: VV, HPN. Model simulation: HPN. Analysis: HPN and VV. Manuscript preparation: HPN and GN taking input from all the authors. All authors read and approved the final manuscript.

Funding

Authors acknowledge support from the DST-SPLICE climate change program through project code DST/CCP/NUC/148/2018.

Availability of data and materials

The processed simulation datasets and materials used in this study are available upon request to the corresponding author (hpnayak@ucla.edu). The hourly surface temperature observation at Bhubaneswar airport station is available <https://zenodo.org/deposit/8401193>. The population dataset used is obtained from open source and is available at "<https://www.worldpop.org/>". The initial and boundary conditions for the model is obtained from NCEP-FNL (<https://rda.ucar.edu/datasets/ds083.2>) and the land use land cover for the model is obtained from ISRO-Bhuvan (<https://bhuvan-app3.nrsc.gov.in/data/download/index.php>).

Declarations

Competing interests

The authors do not have any financial or non-financial conflict of interest.

Received: 4 October 2023 Revised: 11 November 2023 Accepted: 4 December 2023

Published online: 20 December 2023

References

- Anasuya, B., Swain, D., & Vinoj, V. (2019). Rapid urbanization and associated impacts on land surface temperature changes over Bhubaneswar Urban District, India. *Environmental Monitoring and Assessment*, 191, 790. <https://doi.org/10.1007/s10661-019-7699-2>
- Arnfield, A. J. (2003). Two decades of urban climate research: A review of turbulence, exchanges of energy and water, and the urban heat island. *International Journal of Climatology*, 23, 1–26.
- Arnfield, J., Herbert, J. M., & Johnson, G. T. (1998). A numerical simulation investigation of urban canyon energy budget variations. Proceedings of 2nd AMS urban environment symposium, Albuquerque, New Mexico, November 2–7, American Meteorological Society, pp. 2–5.
- Block, A., Keuler, K., & Schaller, E. (2004). Impacts of anthropogenic heat on regional climate patterns. *Geophysical Research Letters*, 31, L12211.
- Bougeault, P., & Lacarrere, P. (1989). Parameterization of orography-induced turbulence in a Mesobeta-scale model. *Monthly Weather Review*, 117,

- 1872–1890. [https://doi.org/10.1175/1520-0493\(1989\)117%3c1872:POOIT%3e2.0.CO;2](https://doi.org/10.1175/1520-0493(1989)117%3c1872:POOIT%3e2.0.CO;2)
- Brutsaert, W. (1975). On a derivable formula for long-wave radiation from clear skies. *Water Resources Research*, 11(5), 742–744. <https://doi.org/10.1029/WR011i005p00742>
- Cao, M., & Lin, Z. (2014). Impact of urban surface roughness length parameterization scheme on urban atmospheric environment simulation. *Journal of Applied Mathematics*, D, 267683. <https://doi.org/10.1155/2014/267683>
- Chen, F., Kusaka, H., Tewari, M., Bao, J., & Hirakuchi, H. (2004). Utilizing the coupled WRF/LSM/urban modeling system with detailed urban classification to simulate the urban heat island phenomena over the greater Houston area. 5th Conf. On urban environment (Vancouver, BC 23–27 august 2004) paper 9.11.
- Chen, F., et al. (2011). The integrated WRF/urban modelling system: Development, evaluation, and applications to urban environmental problems. *International Journal of Climatology*, 31, 273–288.
- Chen, Y., Naud, C. M., Rangwala, I., Landry, C. C., & Miller, J. R. (2014). Comparison of the sensitivity of surface downward longwave radiation to changes in water vapor at two high elevation sites. *Environmental Research Letters*, 9, 114015.
- Clinton, N., & Gong, P. (2013). MODIS detected surface urban heat islands and sinks: Global locations and controls. *Remote Sensing of Environment*, 134, 294–304.
- Dudhia, J. (1989). Numerical study of convection observed during the winter monsoon experiment using a mesoscale two-dimensional model. *Journal of the Atmospheric Sciences*, 46, 3077–3107.
- Eastin, M. D., Baber, M., Boucher, A., Di Bari, S., Hubler, R., Stimac-Spalding, B., & Winesett, T. (2018). Temporal variability of the char-lotte (sub)urban heat island. *Journal of Applied Meteorology and Climatology*, 57(1), 81–102.
- Estoque, R. C., Murayama, Y., & Myint, S. W. (2017). Effects of landscape composition and pattern on land surface temperature: An urban heat island study in the megacities of Southeast Asia. *Science of the Total Environment*, 577, 349–359.
- Fan, H., & Sailor, D. (2005). Modelling the impacts of anthropogenic heating on the urban climate of Philadelphia: A comparison of implementations in two PBL schemes. *Atmospheric Environment*, 39(1), 73–84. <https://doi.org/10.1016/j.atmosenv.2004.09.031>
- Feldman, D. R., Worden, M., Falco, N., Denny-Frank, P. J., Chen, J., Dafflon, B., & Wainwright, H. (2022). Three-dimensional surface downwelling longwave radiation clear-sky effects in the upper Colorado River basin. *Geophysical Research Letters*, 49, e2021GL094605. <https://doi.org/10.1029/2021GL094605>
- Feng, J.-M., Wang, Y.-L., Ma, Z.-G., & Liu, Y.-H. (2012). Simulating the regional impacts of urbanisation and anthropogenic heat release on climate across China. *Journal of Climate*, 25(20), 7187–7203. <https://doi.org/10.1175/JCLI-D-11-00333.1>
- Gogoi, P. P., Vinoj, V., Swain, D., Roberts, G., Dash, J., & Tripathy, S. (2019). Land use and land cover change effect on surface temperature over eastern India. *Scientific Reports*, 9(1), 1–10.
- Grimmond, S. (2007). Urbanization and global environmental change: Local effects of urban warming. *The Geographical Journal*, 173, 83–88.
- Grover, A., & Singh, R. B. (2015). Analysis of urban Heat Island (UHI) in relation to normalized Difference vegetation index (NDVI): A comparative study of Delhi and Mumbai. *Environments*, 2, 125–138.
- Hong, S.-Y., & Lim, J. O. J. (2006). The WRF single-moment 6-class microphysics scheme (WSM6). *Journal of the Korean Meteorological Society*, 42, 129–151.
- Hunt, J. C., Aktas, Y. D., Mahalov, A., Moustou, M., Salamanca, F., Georgescu, M. (2018). Climate change and growing megacities: Hazards and vulnerability. Proceedings of Institution of Civil Engineers—Engineering sustainability, 314–326.
- Ichinose, T., Shimodono, K., & Hanaki, K. (1999). Impact of anthropogenic heat on urban climate in Tokyo. *Atmospheric Environment*, 33(24), 3897–3909.
- Imhof, M. L., Zhang, P., Wolfe, R. E., & Bounoua, L. (2010). Remote sensing of the urban heat island effect across biomes in the continental USA. *Remote Sensing of Environment*, 114, 504–513.
- IPCC: Climate Change (2007). Synthesis Report. Contribution of Working Groups I, II and III to the Fourth Assessment Report of the Intergovernmental Panel on Climate Change, Core Writing Team, edited by: Pachauri, R. K. & Reisinger, A., IPCC, Geneva, Switzerland, 104 pp., available at: <https://www.ipcc.ch/report/ar4/syr/> 2007.
- IPCC: Climate Change (2014). Synthesis Report. Contribution of Working Groups I, II and III to the Fifth Assessment Report of the Intergovernmental Panel on Climate Change [(eds) Core Writing Team, Pachauri, R. K. & Meyer, L. A.]. 151 (IPCC, Geneva, Switzerland, 2014).
- Jin, M., Dickinson, R. E., & Zhang, D.-L. (2005). The footprint of urban areas on global climate as characterized by MODIS. *Journal of Climate*, 18, 1551–1565.
- Johnson, G. T., Oke, T. R., Lyons, T. J., Steyn, D. G., Watson, I. D., & Voogt, J. A. (1991). Simulation of surface urban Heat Islands under “ideal” conditions at night, part 1: Theory and tests against field data. *Boundary-Layer Meteorology*, 56, 275–294.
- Kain, J. S. (2004). The Kain–Fritsch convective parameterization: An update. *Journal of Applied Meteorology*, 43(1), 170–181.
- Kalnay, E., & Cai, M. (2003). Impact of urbanization and land-use change on climate. *Nature*, 423, 528–531.
- Kaufmann, R. K., Seto, K. C., Schneider, A., Liu, Z., Zhou, L., & Wang, W. (2007). Climate response to rapid urban growth: Evidence of a human-induced precipitation deficit. *Journal of Climate*, 20, 2299–2306.
- Kishtawal, C. M., Niyogi, D., Tewari, M., Pielke, R. A., Sr., & Shepherd, J. M. (2010). Urbanization signature in the observed heavy rainfall climatology over India. *International Journal of Climatology*, 30(13), 1908–1916.
- Kusaka, H., & Kimura, F. (2004). Coupling a single-layer urban canopy model with a simple atmospheric model: Impact on urban heat island simulation for an idealized case. *Journal of the Meteorological Society of Japan*, 82, 67–80. <https://doi.org/10.2151/jmsj.82.67>
- Kusaka, H., Kondo, H., Kikegawa, Y., & Kimura, F. (2001). A simple single layer urban canopy model for atmospheric models: Comparison with multi-layer and slab models. *Boundary-Layer Meteorology*, 101, 329–358.
- Li, X., Mitra, C., Dong, L., & Yang, Q. (2018). Understanding land use change impacts on microclimate using weather research and forecasting (WRF) model. *Physics and Chemistry of the Earth*, 103, 115–126.
- Li, X. X., Koh, T. Y., Panda, J., & Norford, L. K. (2016). Impact of urbanization patterns on the local climate of a tropical city, Singapore: An ensemble study. *Journal of Geophysical Research-Atmospheres*, 121, 4386–4403.
- Li, Z., Chan, J. C. L., Zhao, K., & Chen, X. (2021). Impacts of urban expansion on the diurnal variations of summer monsoon precipitation over the South China coast. *Journal of Geophysical Research-Atmospheres*, 126, e2021JD035318. <https://doi.org/10.1029/2021JD035318>
- Ma, S., Pitman, A., Hart, M., Evans, J. P., Haghdad, N., & MacGill, I. (2017). The impact of an urban canopy and anthropogenic heat fluxes on Sydney’s climate. *International Journal of Climatology*, 37, 255–270.
- Mahmood, R., et al. (2010). Impacts of land use/land cover change on climate and future research priorities. *Bulletin of the American Meteorological Society*, 91, 37–46.
- Masson, V. (2000). A physically-based scheme for the urban energy budget in atmospheric models. *Boundary-Layer Meteorology*, 94, 357–397.
- Meili, N., Paschalis, A., Manoli, G., & Faticchi, S. (2022). Diurnal and seasonal patterns of global urban dry islands. *Environmental Research Letters*, 17, 054044.
- Miao, S., Chen, F., Lemone, M. A., Tewari, M., Li, Q., & Wang, Y. (2009). An observational and modeling study of characteristics of urban heat island and boundary layer structures in Beijing. *Journal of Applied Meteorology and Climatology*, 48, 484–501.
- Mills, G. M. (1993). Simulation of the energy budget of an urban canyon – 1. Model structure and sensitivity test. *Atmospheric Environment*, 27B, 157–170.
- Mlawer, E. J., Taubman, S. J., Brown, P. D., Iacono, M. J., & Clough, S. A. (1997). Radiative transfer for inhomogeneous atmospheres: RRTM, a validated correlated-k model for the longwave. *Journal of Geophysical Research*, 102(D14), 16,663–16,682.
- Mohan, M., & Kandya, A. (2015). Impact of urbanization and land-use/land-cover change on diurnal temperature range: A case study of tropical urban airshed of India using remote sensing data. *Science of The Total Environment*, 506–507, 453–465.
- Mohan, M., Singh, V., Bhati, S., Lodhi, N., Sati, A., Sahoo, N. R., Dash, S., Mishra, P., & Dey, S. (2020). Industrial heat island: A case study of Angul-Talcher region in India. *Theoretical and Applied Climatology*, 141. <https://doi.org/10.1007/s00704-020-03181-9>
- Mohan, M., et al. (2012). Urban Heat Island assessment for a tropical urban Airshed in India. *Atmospheric and Climate Sciences*, 02, 127–138.

- Morris, K. I., Chan, A., Salleh, S. A., Ooi, M. C. G., Oozeer, M. Y., & Abakr, Y. A. (2016). Numerical study on the urbanisation of Putrajaya and its interaction with the local climate, over a decade. *Urban Climate*, 16, 1–24.
- Nandini, G., Vinoj, V., Sethi, S. S., et al. (2022). A modelling study on quantifying the impact of urbanization and regional effects on the wintertime surface temperature over a rapidly-growing tropical city. *Computational Urban Science*, 2, 40. <https://doi.org/10.1007/s43762-022-00067-6>
- Narumi, D., Kondo, A., & Shimoda, Y. (2009). Effects of anthropogenic heat release upon the urban climate in a Japanese megacity. *Environmental Research*, 109, 421–431.
- National Remote Sensing Centre, India, 2008. National Land Use and Land Cover Mapping Using Multi-Temporal AWIFS Data: NRSA/LULC/1:250K/2008–3.
- Naud, C. M., Chen, Y., Rangwala, I., & Miller, J. R. (2013). Sensitivity of downward longwave surface radiation to moisture and cloud changes in a high-elevation region. *Journal of Geophysical Research – Atmospheres*, 118. <https://doi.org/10.1002/jgrd.50644>
- Nayak, S., & Mandal, M. (2012). Impact of land-use and land-cover changes on temperature trends over Western India. *Current Science*, 102, 1166–1173.
- Niu, G.-Y., et al. (2011). The community Noah land surface model with multi-parameterization options (Noah-MP): 1. Model description and evaluation with local-scale measurements. *Journal of Geophysical Research*, 116, D12109. <https://doi.org/10.1029/2010JD015139>
- Niyogi, D., Osuri, K. K., Busireddy, N. K. R., & Nadimpalli, R. (2020). Timing of rainfall occurrence altered by urban sprawl. *Urban Climate*, 33, 10064.
- Niyogi, D., et al. (2018). In K. P. Vadrevu, T. Ohara, & C. Justice (Eds.), *In land-atmospheric research applications in south and Southeast Asia* (pp. 553–575). Springer International Publishing. https://doi.org/10.1007/978-3-319-67474-2_25
- Oke, T. R. (1973). City size and the urban heat island. *Atmospheric Environment*, 7, 769–779.
- Patel, P., Jamshidi, S., Nadimpalli, R., Aliaga, D. G., Mills, G., Chen, F., et al. (2022). Modeling large-scale heatwave by incorporating enhanced urban representation. *Journal of Geophysical Research-Atmospheres*, 127, e2021JD035316. <https://doi.org/10.1029/2021JD035316>
- Peng, S., et al. (2012). Surface urban heat island across 419 global big cities. *Environmental Science & Technology*, 46, 696–703.
- Pielke, R. A., Sr., Pitman, A., Niyogi, D., Mahmood, R., McAlpine, C., Hossain, F., Goldewijk, K. K., Nair, U., Betts, R., Fall, S., & Reichstein, M. (2011). Land use/land cover changes and climate: Modeling analysis and observational evidence. *Wiley Interdisciplinary Reviews: Climate Change*, 2(6), 828–850.
- Pluss, C., & Ohmura, A. (1997). Longwave radiation on snow-covered mountainous surfaces. *Journal of Applied Meteorology*, 36, 818–824 <https://journals.ametsoc.org/view/journals/apme/36/6/1520-0450-36.6.818.xml>
- Reynolds, C. A., Jackson, T. J., & Rawls, W. J. (2000). Estimating soil water-holding capacities by linking the food and agriculture organization soil map of the world with global pedon databases and continuous pedo-transfer functions. *Water Resources Research*, 36, 3653–3662.
- Ruckstuhl, C., Philipona, R., Morland, J., & Ohmura, A. (2007). Observed relationship between surface specific humidity, integrated water vapor, and longwave downward radiation at different altitudes. *Journal of Geophysical Research*, 112, D03302. <https://doi.org/10.1029/2006JD007850>
- Sharma, A., Wuebbles, D. J., & Kotamarthi, R. (2021). The need for urban-resolving climate modelling across scales. *AGU Advances*, 2, e2020AV000271. <https://doi.org/10.1029/2020AV000271>
- Skamarock, W. C. et al. (2008). A description of the advanced research WRF version 3, NCAR Technical Note 1–113.
- Sugawara, H., & Takamura, T. (2006). Longwave radiation flux from an urban canopy: Evaluation via measurements of directional radiometric temperature. *Remote Sensing of Environment*, 104, 226–237.
- Swain, D., Robert, G. J., Dash, J., Lekshmi, K., Vinoj, V., & Tripathy, S. (2017). Impact of rapid urbanization on the City of Bhubaneswar, India. *Proceedings of the National Academy of Sciences, India, Section A: Physical Sciences*, 87, 845–853.
- Swain, M., Nadimpalli, R. R., Mohanty, U. C., Guhathakurta, P., Gupta, A., Kaginalkar, A., Chen, F., & Niyogi, D. (2023). Delay in timing and spatial reorganization of rainfall due to urbanization- analysis over India's smart city Bhubaneswar. *Computational Urban Science*. <https://doi.org/10.1007/s43762-023-00081-2>
- United Nations. (2015). *World urbanization prospects: The 2014 revision, (ST/ESA/SER.A/366)*. Department of Economic and Social Affairs, Population Division.
- Wang, L., Sun, T., Zhou, W., Liu, M., & Li, D. (2023). Deciphering the sensitivity of urban canopy air temperature to anthropogenic heat flux with a forcing-feedback framework. *Environmental Research Letters*, 18. <https://doi.org/10.1088/1748-9326/ace7e0>
- Wang, Y., Zhang, G. J., Gong, P., Dickinson, R. E., Fu, R., Li, X., et al. (2021). Winter warming in North America induced by urbanization in China. *Geophysical Research Letters*, 48, e2021GL095465. <https://doi.org/10.1029/2021GL095465>
- Wu, W., Li, L., & Li, C. (2021). Seasonal variation in the effects of urban environmental factors on land surface temperature in a winter city. *Journal of Cleaner Production*, 299, 1–9.
- Yang, P., Ren, G., & Liu, W. (2013). Spatial and temporal characteristics of Beijing urban heat island intensity. *Journal of Applied Meteorology and Climatology*, 52(8), 1803–1816.
- Zhang, N., Wang, X., Chen, Y., Dai, W., & Wang, X. (2016). Numerical simulations on influence of urban land cover expansion and anthropogenic heat release on urban meteorological environment in Pearl River Delta. *Theoretical and Applied Climatology*, 126, 469–479.
- Zhao, L., Lee, X., Smith, R. B., & Oleson, K. (2014). Strong contributions of local background climate to urban heat islands. *Nature*, 511, 216–219.
- Zhong, S., Qian, Y., Zhao, C., Leung, R., Wang, H., Yang, B., Fan, J., Yan, H., Yang, X. Q., & Liu, D. (2017). Urbanization-induced urban heat island and aerosol effects on climate extremes in the Yangtze River Delta region of China. *Atmospheric Chemistry and Physics*, 17(8), 5439–5457.
- Zhong, S., & Yang, X. Q. (2015). Ensemble simulations of the urban effect on a summer rainfall event in the great Beijing metropolitan area. *Atmospheric Research*, 153, 318–334.
- Zhou, B., Rybski, D., & Kropp, J. P. (2013). On the statistics of urban heat island intensity. *Geophysical Research Letters*, 40, 5486–5491.
- Zhou, L., Dickinson, R. E., Tian, Y., Fang, J., Li, Q., Kaufmann, R. K., Tucker, C. J., & Myneni, R. B. (2004). Evidence for a significant urbanization effect on climate in China. *Proceedings of the National Academy of Sciences*, 101, 9540–9544.

Publisher's Note

Springer Nature remains neutral with regard to jurisdictional claims in published maps and institutional affiliations.